fractal and fractional

MDPI

Article

Research on Fractal Evolution Characteristics and Safe Mining Technology of Overburden Fissures under Gully Water Body

Kaijun Miao, Shihao Tu *, Hongsheng Tu *, Xun Liu, Wenlong Li, Hongbin Zhao, Long Tang, Jieyang Ma and Yan Li

State Key Laboratory of Coal Resources and Safe Mining, School of Mines, China University of Mining and Technology, Xuzhou 221116, China

* Correspondence: tsh@cumt.edu.cn (S.T.); 5536@cumt.edu.cn (H.T.); Tel.: +86-139-5216-0512 (S.T.)

Abstract: A fractal realizes the quantitative characterization of complex and disordered mining fracture networks, and it is of great significance to grasp the fractal characteristics of rock movement law to guide mine production. To prevent the water-conducting fracture (WF) under the gullies from conducting the surface water body, and to realize the purpose of safe production and surface water body protection. The evolution of overburden fissures in the working face with shallow buried gulley landform and thick bedrock conditions is studied. The development height of water-conducting fracture (DHWF) is theoretically analyzed. The evolution characteristics of overlying fissures with different mining heights were observed by similarity simulation, and the observation results were analyzed by fractal theory. The results show that the main factor that determines the height of WF is mining height. The working face is mined at different mining heights, and the corresponding indexes such as the height of the WF, the area of the caving zone and the fractal dimension are related to engineering phenomena. In particular, the appearance and disappearance of the separation space correspond to the fractal dimension fluctuation phase. The safe mining technology under a gully water body, which mainly reduces mining height, is adopted, and the fissures of the working face are not connected to the surface water body after mining.

Keywords: fissure evolution; fractal feature; gully landform; similarity simulation; water conservation mining; height reduction mining

check for updates

Citation: Miao, K.; Tu, S.; Tu, H.; Liu, X.; Li, W.; Zhao, H.; Tang, L.; Ma, J.; Li, Y. Research on Fractal Evolution Characteristics and Safe Mining Technology of Overburden Fissures under Gully Water Body. *Fractal Fract.* **2022**, *6*, 486. https://doi.org/10.3390/fractalfract6090486

Academic Editors: Alexandre G. Evsukoff and Wojciech Sumelka

Received: 13 July 2022
Accepted: 28 August 2022
Published: 30 August 2022

1. Introduction

In recent years, the focus of China's coal production has gradually shifted to the west. The Shendong mining area is an important energy base. The coal seam is characterized by shallow burial depth and good occurrence conditions and is suitable for large-scale mechanized mining. According to the topographic features, the area is mainly divided into loess gully area and aeolian sand area. In the loess gully area, many gullies are formed due to the accumulation and erosion of surface runoff [1–3]. When fully mechanized mining is carried out under gully landforms with large changes in buried depth, the surface water body in the gully is closest to the coal seam, and the fissures formed by mining can easily conduct surface water, resulting in mine water inrush and surface water damage [4–6]. To ensure the safety of the working face over the gully, it is necessary to study the evolution characteristics of the overburden fissures.

Since the surface gully landforms in the western mining area account for more than 90% [1], the ecological environment is fragile and water resources are scarce [7,8], a lot of research work has been carried out on the gully landforms and water conservation mining. There are differences in the activities and control of the bedrock type and the sandy soil type gully slope. The selection of the support needs to consider the intensity and sequence of the occurrence of rock pressure in each stage of the gully [9]. Under this feature of mining-induced pressure, overlying strata movement and fracture development also show new features [10,11]. With the condition of thin bedrock, the mining fissures of shallow buried coal seams generally develop to the surface, and the bench fracture occurs on the surface. Generally, field measurements and similar simulations are used to study the main composition of overlying fissures and the distribution of surface fissures [12].

Due to the complexity and randomness of the development of overlying fissures, and the "black box" characteristics of overlying strata movement, it is often difficult to observe through actual measurements [13,14]. In 1967, Dr. Mandelbrot proposed the fractal theory, which is widely used to describe rough and irregular phenomena in nature [15]. Xie established fractal rock mechanics and found that the fissures of the mining rock mass have good fractal characteristics, and the fissure network of the overlying rock has the characteristics of increasing dimension with advancing of the working face [16,17]. The fracture network of the overlying rock in deep mining is affected by the dimensionality reduction and calculated by the fractal dimension ratio of the three zones [18]. The dissipative structure characteristics of the overlying fissure system were expounded and believed that the fractal dimension sudden increase corresponds to the breaking of the key layer of the overlying rock, which is consistent with the random fluctuation characteristics of the dissipative structure system order [19]. The fractal dimension of the overlying fissures in the mining process of the working face has a jump, and the nonlinear relationship between the fractal dimension, the separation layer, and the surface subsidence is preliminarily regressed [20]. The above studies show that the current research on the fractal study of the gully landform features of mineral pressure and overlying fissures has been carried out separately, but there are few studies on the relationship between the fractal dimensional characteristics of the gully landform mining overburden fissures and rock formation control.

In this paper, taking an approximate shallow buried coal seam in Shendong mining area as the study site, to ensure the safe mining of the working face under the water body in the gully, the method of theoretical analysis and similar simulation is used to study the evolution characteristics of the overburden fissures. The fractal geometry and digital image processing tools are used to quantitatively describe and analyze the evolution process of mining fissures. The fractal characteristics of mining height on the evolution of overlying fissures were obtained, and the fractal dimension, caving zone height, water-conducting fissure development height, caving zone area, fissure network area, and rock formation in the mining process were summarized. The correlation of movement laws provides theoretical support for low-damage mining and water-preserving mining.

2. Engineering Background

The research mine is located in the Shendong mining area, and the average mining depth of the working face is 160 m. In the overlying rock, the bedrock is about 150 m, and the loose layer is 10 m. The average thickness of the 2-2 coal seam is about 4.0 m, and the dip angle is 1~3°. The surface of the mine field belongs to the plateau erosive hilly landform, the overlying Quaternary loess is thin, and the bedrock is exposed in large areas on the surface and in the valley. There are four aquifers in the overlying rock, which will have little impact on production after drilling. This area is a semi-arid and semi-desert area. Although there is no lake in the mine field, there will be a short torrent after the rain due to the concentrated rainfall. Under the action of erosion, the gully develops, and there are usually streams. The largest water-bearing gully in the mine field is Naogou, which is located above the P101, with a depth of about 40 m and a width of about 100 m (Figure 1). Due to the large water content of the gullies, the WF can easily reach the bottom of the gullies during the mining process of the first working face P101, resulting in water inrush accidents. Studying the evolution characteristics of overlying fissures under these conditions is an urgent need for the safe mining of working faces and water resources protection in fragile ecological mining areas.

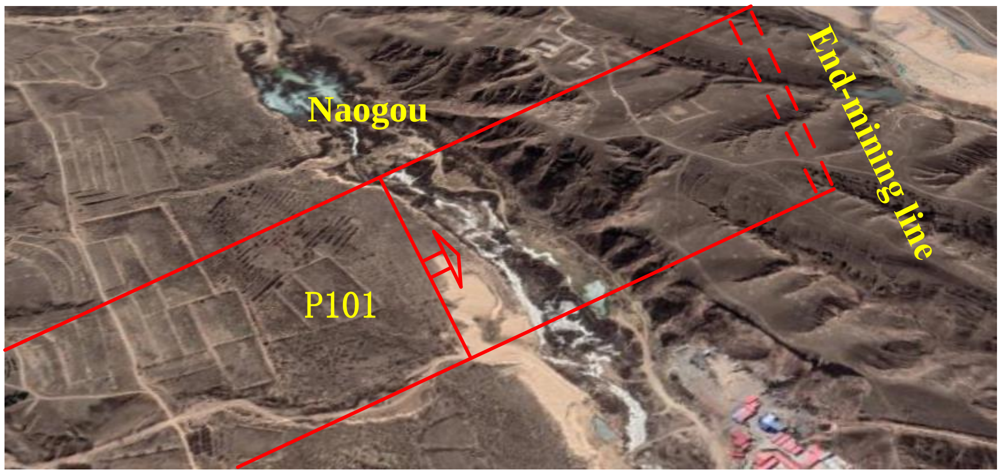

Figure 1. Distribution of working face P101 and gully.

3. Analysis of DHWF

3.1. Overview of the Equation for Predicting DHWF

To avoid water inrush accidents caused by mining under gully water bodies, it is necessary to analyze the factors that cause water inrush accidents. Affected by the superposition of gully and shallow burial factors, gully has become a weak link for the conduction of overburden fissures in working face mining. Therefore, it is necessary to predict the development height of WF under this condition to ensure that the overlying strata fissures do not conduct the water flow in the gullies after mining. The analysis of DHWF is generally obtained through empirical equations, theoretical analysis, numerical simulation, physical simulation, and field-testing methods. Due to the convenience of the equation prediction method, many regression prediction equations for DHWF have been obtained. The most widely used equation for predicting DHWF comes from "Regulations for Setting Coal Pillar and Mining Pressed Coal Under Buildings, Water Bodies, Railways, and Main Roadways in China" (hereinafter referred to as the "Regulations") [21].

$$H_{li} = \frac{100\sum M}{c_1\sum M + c_2} \pm c_3 \tag{1}$$

$$H_{li} = c_4\sqrt{\sum M} + c_5 \tag{2}$$

where H_{li} is DHWF, m; M is the mining height, m; c_i is the coefficient that depend on strata lithology (Table 1).

Table 1. Selection of coefficients in the equation for predicting DHWF.

Lithology of Direct Roof	c_1	c_2	c_3	c_4	c_5
Hard	1.2	2.0	8.9	30	10
Medium hard	1.6	3.6	5.6	20	10
Soft and weak	3.1	5.0	4.0	10	5
Extremely weak	5.0	8.0	3.0	-	-

The equation for predicting DHWF in the shallow-buried coal seam with a thick loose layer and thin bedrock based on the measured statistics [22]:

$$H_{li} = \frac{100\sum M}{1.6\sum M + 2.2} \pm 5.6 \tag{3}$$

The statistical empirical equation for the height of the WF obtained by a large number of mines in the Yushenfu mining area, the coefficient $k \in (21, 30)$ in the equation, and the average value of 26 is often taken in engineering [23]:

$$H_{li} = kM \tag{4}$$

Comprehensively considering the production geological conditions of the western mine, including coal seam mining height, working face length, working face mining speed, overburden structure coefficient and working face burial depth, etc., based on the measured data of 37 mines, the height of the WF prediction model was established by regression [24]:

$$H_{li} = 36.67 + [5.46 + 0.18\ln(L - 89.99) + 5.22b - 1.22\ln V + 1.02\ln(H + 30.18)]M \tag{5}$$

Combined with the actual production, the working face inclination length L is determined according to the equipment conditions, and the reduction will significantly reduce the economics of mining. The hard rock proportion coefficient b and the burial depth H are objective conditions. Therefore, it can be considered to reduce the development height of the overlying fissures from the perspective of mining parameters. In the actual production of Selian Coal Mine, L is the length of the working face, which is 280 m; H is the mining depth, which is 160 m; b is the proportion coefficient of hard rock, and the calculation equation is as follows:

$$b = \frac{\sum h}{nM} \tag{6}$$

Σh is the cumulative total thickness of the hard rock in the overlying rock, n is the empirical proportional coefficient, and 20 is taken into account for considering the safety factor. M is the mining height. Accordingly, Equation (6) is substituted into Equation (5), and all known production geological data of Selian Coal Mine are substituted to obtain the equation for predicting DHWF:

$$H_{li} = 51.8 + (11.75 - 1.22\ln V)M \tag{7}$$

V is the daily mining speed of the working face, which is 4~20 m according to the production organization and equipment capacity, and the mining height M is 2.5~5.0 m. The characteristics of DHWF affected by the two factors of mining speed and mining height under the conditions of the Selian Coal Mine are shown in Figure 2.

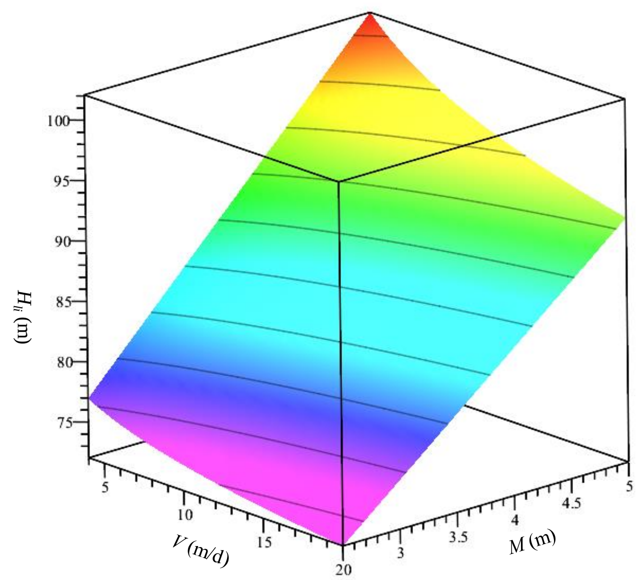

Figure 2. Influence characteristics of two factors in the prediction equation of DHWF in Selian Coal Mine.

It can be seen from Figure 2 that, compared with the mining height, the mining speed of the working face has less influence on DHWF. Whether it is the traditional WF height prediction equation or the multivariate statistical regression's WF height prediction equation, it can be concluded that mining height is a key factor affecting the WF height. However, the applicability of the WF height prediction equation to this project needs further analysis.

3.2. Applicability Analysis

Based on the above-mentioned prediction equation for the height of WF, the comparative analysis is shown in Figure 3. The mining height of the research working face is 4.0 m, and the roof is weak. The predicted heights of the roof WF are shown in Table 2, respectively.

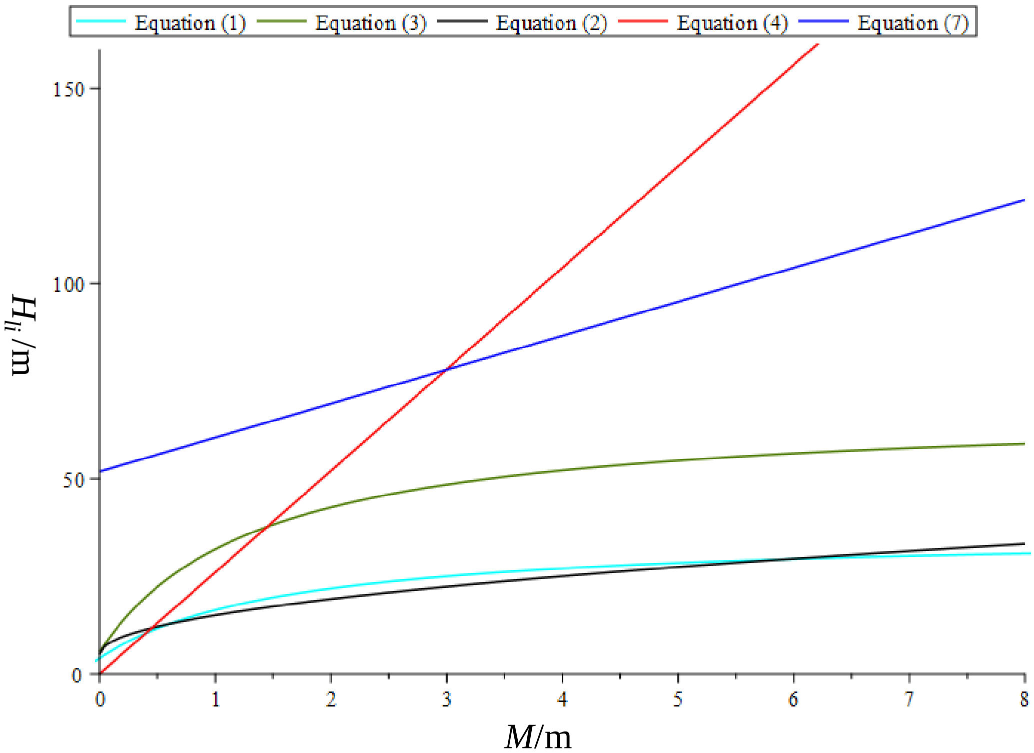

Figure 3. Comparison of equations for predicting DHWF.

Table 2. Development height of WF.

Equation	(1)	(2)	(3)	(4)	(7) *
DHWF/m	26.8	25.0	52.1	84~120	86.6

* In Equation (7), the mining speed V is taken as 12 m, and the corresponding water-conducting fracture zone height is 86.6 m.

The expected results of Equations (1) and (2) in the regulations are similar, and the maximum value is 33.3 m when the mining height is 8 m. Since the measured samples are from the fully mechanized mining face in China at the end of the last century, it is suitable for the stratified mining height of 1~3 m. Layered mining of thick coal seams. The form of Equation (3) is the same as that in the regulations. When the mining height is 8 m, the height of the WF is 58.9 m, which is a beneficial correction in the development of coal mining technology and is suitable for hard roof conditions. value is too small. Fan measured the height of the WF in the Yushen mining area and the Shendong mining area, and the empirical equation for the height of the WF obtained by statistics is similar to the research object due to the mining height, geological conditions, and layout of the working face and roadway. The results are expected to be more reliable. Under the condition of a mining height of 4.0 m, it is estimated that the height of the maximum WF is 120 m, and there is a threat of fracture conduction to the surface water body in the mining area with an average buried depth of 160 m and a gully depth of 38 m. Under the conditions of this mine, the predicted value of the WF height of the equation of the multivariate statistical regression is similar to the lower limit of Fan's empirical equation. At the same time, it can be seen from the figure that most of the mining heights less than 3 m have no practical significance. The reason for this is that the minimum mining height in the regression sample is 2.2 m.

3.3. Optimization of Mining Parameters

To ensure safe mining under the gullies, a reasonable thickness of the protective layer should be selected for the upper part of the water-conducting fissures. According to the Regulations, the mine is a loose layer with no clay layer at the bottom and weak roof conditions, and the thickness of the protective layer is 5 times higher. The thickness H_J of the overlying rock strata is as shown in Equation (8):

$$H_J = H_{li} + 5M = K_J M \tag{8}$$

In the equation, K_J is the water-resistance coefficient of the bedrock, which is taken as 26~35. In the study, H_J is taken as 110 m under the gully of the mine, and the maximum value of K_J is taken as 35 in consideration of safety, and M is calculated to be 3.14 m. Combined with the equipment conditions of the working face, the actual mining height is determined to be 3.20 m.

4. Experimental Study on Fracture Evolution with Different Mining Heights

4.1. Scale Models

The formation and distribution of mining fissures are very complex, and the field measurement can only detect the development position of water-conducting fissures in some areas, and it is difficult to observe and describe the overlying fissures comprehensively. At the same time, because of the high cost of field measurement, similar simulations are widely used at home and abroad to observe the evolution of mining fractures in overlying rocks [25,26].

The average coal seam thickness of the P101 working face is 4.0 m, the coal seam dip is 1~3°, the overlying bedrock is 150 m thick, the slope angle of the gully in the mine field is about 50°, the vertical depth is 38 m, and the bottom width of the gully is 31 m. The physical simulation experiment design is carried out according to the on-site mining conditions and laboratory test conditions. According to the similarity principle, the geometric similarity ratio is C_l = 100, the bulk density similarity constant is C_γ = 1.85, the stress similarity constant is C_σ = $C_l C_\gamma$ = 185, and the time similarity constant is C_t = 10. The size of the simulation project: the length × height is 250 m × 175 m, and the model size: the length × width × height is 2.50 m × 0.30 m × 1.75 m. By laying two identical physical models in parallel, the evolution law of overburden fissures in trench mining was simulated with a mining height of 4.0 cm and a mining height of 3.2 cm, respectively. When simulating the mining of the working face, considering the boundary effect, 25 cm of boundary coal pillars were left at each end of the model, the designed excavation step was 10 cm, and the mining was performed once every 30 min. The material ratio of each rock formation in the physical simulation study is shown in Table 3.

Table 3. Material ratio of physical simulation.

Model Layer *	Lithology	Layer Height/cm	Sand/kg	$CaCO_3$/kg	Gypsum/kg	Water/kg	n *
F2	medium-grained sandstone	10	217.2	21.7	50.7	32.2	1
F1	sandy mudstone	3	64.1	5.3	5.3	8.3	1
C	2-2 coal seam	4	86.1	12.1	5.2	11.5	1
R1	mudstone	0.6	12.7	1.3	0.5	1.6	1
R2(H)	medium and fine-grained sandstone	3	64.1	7.5	3.2	8.3	2
R3	sandy mudstone	14.4	312.0	23.4	54.6	43.3	8
R4(H)	coarse sandstone	8.5	183.6	12.2	28.6	24.9	4
R5	sandy mudstone	5	108.3	13.5	13.5	15.0	3
R6	mudstone	5	107.6	15.1	6.5	14.4	3
R7(H)	coarse sandstone	8.5	183.6	12.2	28.6	24.9	4
R8	sandy mudstone	8	172.8	19.2	19.2	23.5	4
R9(H)	siltstone	6	130.0	9.7	22.7	18.1	3
R10	mudstone	6	128.3	15.0	6.4	16.6	3
R11(H)	siltstone	8	172.8	11.5	26.9	23.5	4
R12	sandy mudstone	9	194.4	21.6	21.6	26.4	4
R13(H)	siltstone	8	172.8	11.5	26.9	23.5	4
R14	sandy mudstone	6	129.6	14.4	14.4	17.6	3
R15(H)	siltstone	8	172.8	11.5	26.9	23.5	4
R16	mudstone	6	128.3	15.0	6.4	16.6	3
R17	conglomerate	10	211.1	18.5	7.9	26.4	4
R18(H)	coarse sandstone	8	150.9	7.5	17.6	19.6	3
R19	sandy mudstone	12	212.7	21.3	21.3	28.4	5
R20	fine sandstone	10	158.2	15.8	6.8	20.1	3
R21	sand, gravel	8.2	118.2	6.6	6.6	14.6	2

* In the first column, R represents roof, F represents floor, C represents coal, H represents hard rock, and n represents the number of re-layers.

4.2. Fractal Calculation Method and Results of Mining Fracture Network

The two models were excavated step by step to observe the evolution law of overlying fissures. The distribution results of the overlying fissures were recorded by a high-definition camera, and the fractal calculation of the recorded results was carried out with the help of the fractal calculation software Fraclab. Fraclab is a signal and image processing plugin based on fractal and multifractal methods, embedded in Matlab. The fractal dimension calculation adopts the Box-counting method, whereby the fractal graph is placed on a uniformly divided grid, and the statistical graph covers the variation of the grid number by dividing the grid at different scales. Fractal dimension calculation adopts:

$$Dim_{box}(S) = \lim_{r \to 0} \frac{\log N(r)}{\log(1/r)} \tag{9}$$

where $N(r)$ is the number of grids occupied by the target image S under the measurement r.

The analysis method flow and partial results of fractal characteristics and evolution law of overlying fissures are shown in Figure 4. The calculation accuracy of the software is tested by using the Sierpinski triangle image of the same pixel. The calculated fractal dimension is 1.5789 and the theoretical value is 1.58, which meets the calculation accuracy. For the recorded pictures of the overlying fissures under different excavation steps, since there are generally marked points on the surface of similar simulation experiments, after removing the interference points with Photoshop software. The Crack Information Analysis System (CIAS) for analyzing fractures was developed by the group of Prof. Chao-Sheng Tang [27,28]. The pictures are imported into CIAS which runs on Matlab. The pictures are converted into matrix data, and the matrix data is converted into matrix data by the binarization function. The binarized image is processed by noise reduction, which can filter out rough cracks and isolated small points in a part of the scale range. Afterwards, the final fracture network can be obtained through the fracture skeleton extraction function. The binary data pictures of the observation results of some overlying fissures with the same excavation step are shown in Table 4.

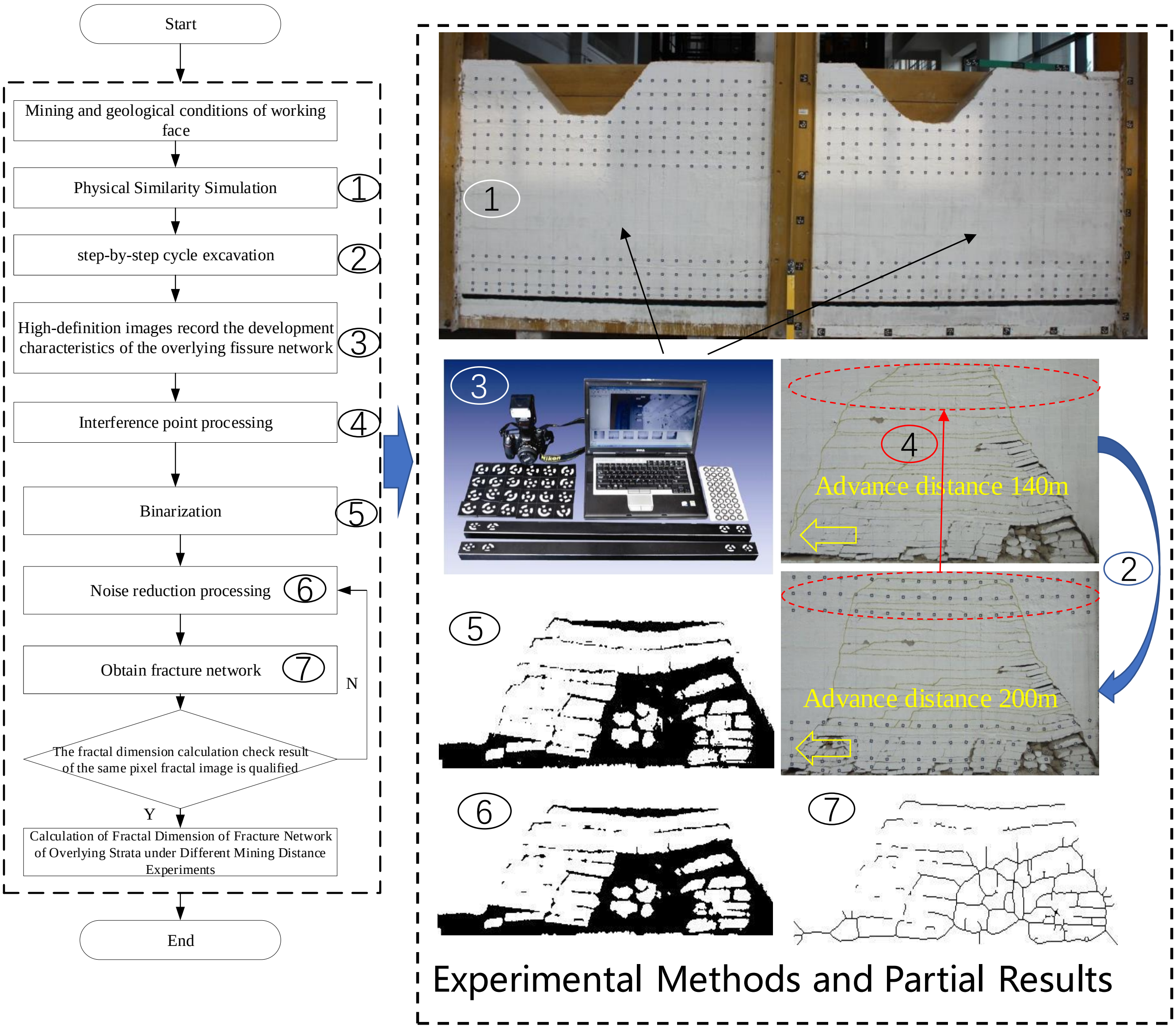

Figure 4. Analysis method flow and partial results of fractal characteristics and evolution law of overlying fissures.

It can be seen from Table 4 that after the overlying rock is destroyed, the developed fissures have an approximate trapezoid shape. The fracture height of the overlying rock increases during the mining process of the working face. When the mining reaches the 200 m position, the model 1 fissure develops but does not lead to the bottom of the gully, and the model 2 fissure has been connected to the gully slope. The results show that reducing the mining height to 3.2 m can realize safe mining under the gully.

Table 4. Extraction of overlying rock fracture network with different mining heights.

s */m	Model 1: Mining Height 3.2 m	Model 2: Mining Height 4.0 m
40	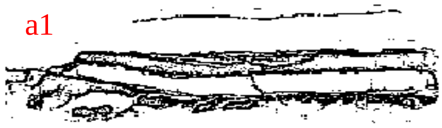	
80		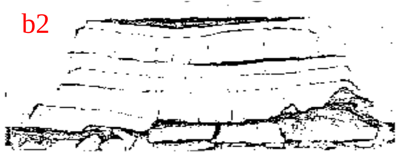
120		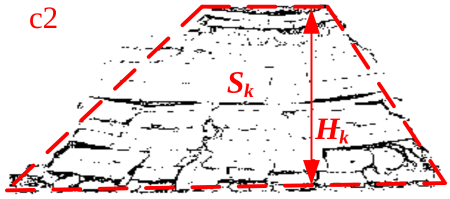
160	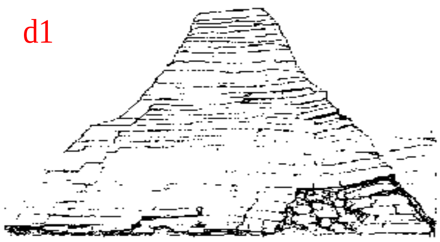	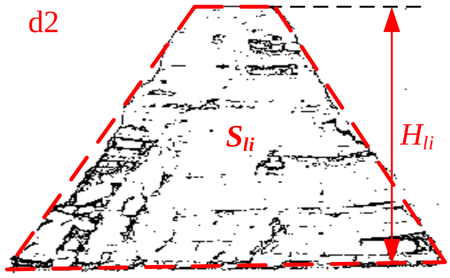
200		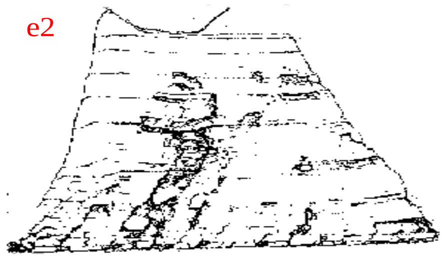

* s is the advance distance of the working face.

4.3. Fractal Characteristics of Overlying Fracture Network Evolution during Height Reduction Mining

To further analyze the evolution characteristics of overburden fissures when mining over the gully under different mining heights, different characteristic parameters of the overburden fissures were selected for analysis. As shown in Figure c2 in Table 4, the height of the caving zone is the range of the overlying rock with a high degree of fragmentation and is the maximum vertical distance H_k from the bottom plate to the top boundary of the horizontal separation space, and the area of the caving zone is approximately S_k. As shown in Figure d2 in Table 4, the DHWF is visible to the naked eye in the overlying rock, the vertical distance H_{li} from the top of the fracture network to the floor, and the area of the water-conducting fracture network is S_{li}.

The fractal dimension of the fissure network in the plane is between 1 and 2. The fractal dimension of the binary data image is calculated by the Fraclab software, and the fractal dimension and caving of the overlying fissure network in the process of the two mining heights and the gully are counted. The height of the belt and the DHWF, the network area of the WF, and the area of the caving zone are estimated, and the eigenvalue laws of the mining fractures of the two models are shown in Figures 5 and 6, respectively.

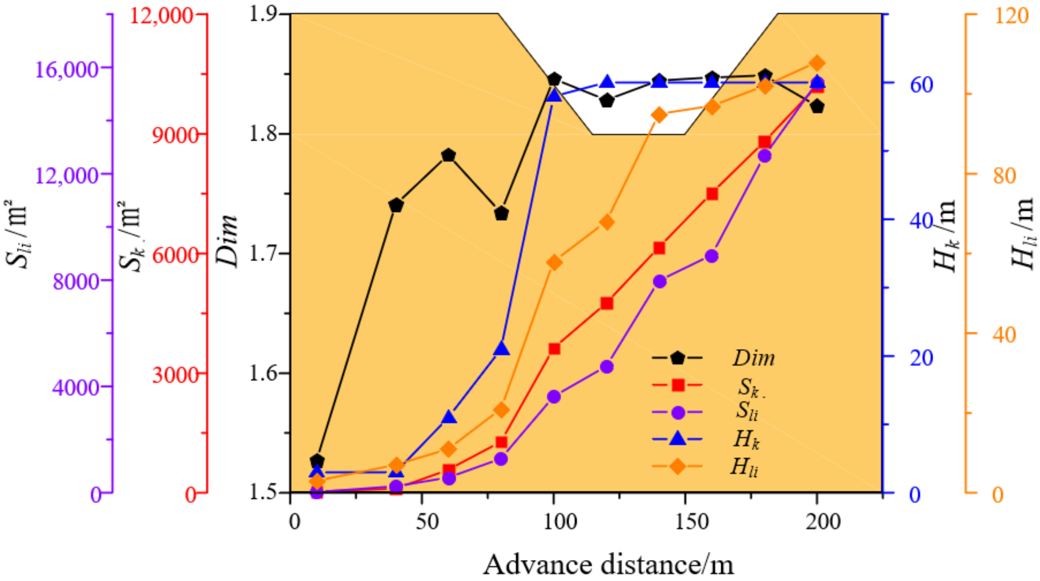

Figure 5. Fractal characteristics of overlying fracture evolution of model 1.

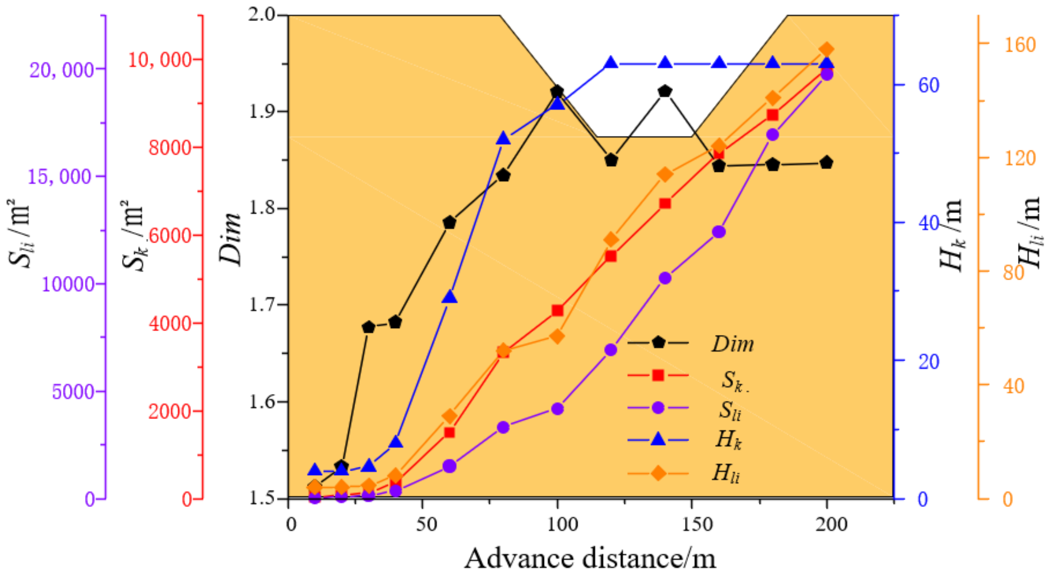

Figure 6. Fractal characteristics of overlying fracture evolution of model 2.

It can be seen from Figure 4 that during the 200 m advanced process of P101, the fractal dimension of the overlying fissure network shows the characteristic of increasing dimension as a whole, and the maximum fractal dimension is 1.82. The height of the caving zone gradually increases with the working face recovery, and gradually stabilizes after advanced to 100 m. After the working face is advanced to 120 m, there is no obvious separation space at the top boundary of the fracture network, and the maximum height of the caving zone is about 60 m. The height of fracture development increases nonlinearly as a whole. Before 100 m of extraction, it is the same as the height of the caving zone. After 140 m of extraction, the growth rate decreases, and it lags behind the extraction position where the separation layer disappears by 20 m. Although the height tends to continue to increase, at the end of the over-groove, the fissure does not reach the gully bottom. Before the extraction of 100 m, the growth law of the caving zone area and the fracture network area is the same. After 100 m of mining, due to the stable height development of the caving zone, the area of the caving zone increases approximately linearly, and the overall growth rate of the fracture network area is greater than that of the caving zone area.

It can be seen from Figure 5 that during the 200 m mining process of P101, the fractal dimension of the overlying fissure network shows the characteristic of increasing dimension as a whole, the maximum fractal dimension is 1.92, and the final fractal dimension is stable at about 1.85. The height of the caving zone increases gradually with the working face recovery and stabilizes at 63 m after being pushed to 120 m, and there is no obvious separation space at the top of the fracture network. The height of fracture development increases in a non-linear relationship as a whole. Before 120 m, the increasing trend of the height of the caving zone is the same. After 120 m, the growth rate decreases, and it also lags behind the 20 m where the separation layer disappears. The DHWF continues to increase, when the working face passed the gully, the fissure has been connected to the bottom and developed to the slope of the gully, and the maximum fissure development height is 158 m. Before 100 m of mining, the growth law of the caving zone area and fracture network area is the same. After 100 m of mining, due to the stable development of caving zone height, the increase of fracture height slows down. The growth rate of the fracture network area is greater than the growth rate of the caving zone area.

The following rules are found by comparing the fracture characteristics of the overlying rock with different mining heights. (1) The change of fractal dimension of shallow overburden fissures can be roughly divided into three stages with the mining of the working face. The first stage is the dimensional ascending stage, whereby the overlying rock collapses to the goaf, the top boundary of the caving zone has obvious separation space, and the growth rate of the development height of the overlying fissures changes from slow to fast, corresponding to 10–60 m in Figure 4 and 10~100 m in Figure 5. The second stage is the fractal fluctuation stage. The separation space of the overlying strata disappeared, the caving zone develops to the maximum height, and the height of the fractures increases rapidly, corresponding to 60–140 m in Figure 4 and 100–160 m in Figure 5. The third stage is the fractal stabilization stage, and the growth rate of the development height of overlying fissures slows down, corresponding to 140–200 m in Figure 4 and 160–200 m in Figure 5. (2) Reducing the mining height of the working face pass the gully can effectively control the development of overlying fissures. The higher the mining height of the working face, the greater the height of the caving zone, the height of the fracture zone, and the fractal dimension of the fracture network under the same mining distance. After the mining height is reduced, the density of the overlying fissures under the gully decreases significantly. (3) With the increase of the mining height, the conductivity of the overlying fissures under the same mining conditions is improved, the degree of disorder of the overlying fissures is higher, and the maximum and stable values of the fractal dimension increase correspondingly, indicating that the fractal dimension can describe the degree of disorder for overlying fissures. (4) The stability of the fractured structure of the key layer of the overlying rock has a significant impact on the fractal dimension of the fracture network. Since there are two siltstone assemblages with an average thickness of more than 20 m in the overlying rock, the fractal dimension of the overlying fissure network fluctuates significantly twice, corresponding to the disappearance of the two closures of the horizontal separation space during the mining process. It is found that in the extraction range of the fractal curve fluctuation, the water-conducting fissure has the largest increasing rate. According to this, it can be proved that the horizontal separation space is the key object for the control of the overlying fissures. However, the generation of the horizontal separation space is periodic, and the control process needs to grasp the appropriate timing. (5) After the mining height was reduced from 4.0 m to 3.2 m, the maximum value of the fractal dimension of the fracture network decreased by 5.5%, the growth rate of the fracture height of the overlying rock slowed down, the fluctuation of the fracture height curve increased, and the mining height decreased 20%. The final fissure development height decreased by 50 m, and the fissure development height decreased by 32%.

5. Safe Mining Technology

As the mining pressure appears more severe than usual when the working face passes through the gully, the overburden damage height may be higher than expected. To avoid the WF conducting the surface water and causing the mine water inrush accident, the following ideas were adopted for crossing the gully at the working face P101: (1) According to the characteristics of climate and precipitation, avoid the rainy season and choose the time when the surface water body freezes in winter to pass the gully. (2) When crossing the gully during non-icing and non-rainy seasons, before mining at the working face, the water body of the surface gullies should be intercepted and transferred for storage, to eliminate the hidden water sources of water inrush within the mining area. The rainy season in study site is concentrated from July to October, and the lowest temperature is from December to January of the following year. The P101 mining is in December when the gullies freeze and have less water. According to the mining influence angle and the position of the gully, the mining plan for reducing the mining height of the working face is determined, as shown in Figure 7.

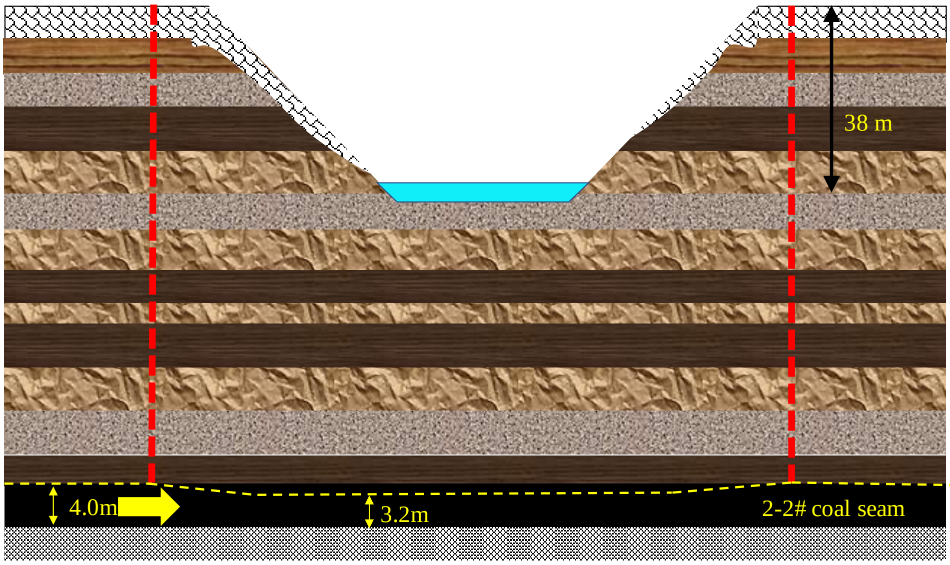

Figure 7. Mining scheme of reducing mining height for P101.

When the working face is mined to a position 10 m before the boundary of the gully, the mining height is gradually reduced from 4.0 m to 3.2 m, and the thickness of the top coal is increased. At the same time, since the hardness and integrity of the coal are significantly greater than those of the mudstone direct roof, the roof coal is used as the roof to improve the situation that the original direct roof is broken, weak, and easy to fall, and indirectly improves the mining speed of the working face. The daily advance distance of the working face is increased from 10.4 m to 17.3 m. According to the predicted Equation (7), the height of the water-conducting fissure zone is 78.3 m. After mining, the water-conducting fissure zone is measured by the drilling fluid loss method to be about 85 m high. The water-conducting fissure zone is not connected to the surface, but the ground fissures still exist. The opening degree of ground fissures decreased from 0.4 m in the non-gully area to about 0.1 m during the mining process.

6. Discussion

The findings of this study clearly show that the mining overburden fissures have fractal characteristics, and the fractal dimension has a good corresponding relationship with the strata movement characteristics. By reviewing the prediction equation of DHWF, it is determined that the mining height of the P101 of Selian Coal Mine under the gully should not exceed 3.2 m. Finally, the protection of the gully water body and the safe mining of working face are realized. Through similar simulations with the same conditions, the evolution characteristics of overlying fissures formed by height reduction mining are intuitively compared. The single index of the DHWF and the fractal characteristics of the fissure network is considered as a whole to judge that the conduction between the water body and the mining space has hysteresis. Some of the issues that emerged from the research are also worth exploring further:

(1) The study site presents the mining conditions of a shallow coal seam, which is different from the fractal characteristics of overlying fissures in many deep coal seams mining [18,20]. The fractal dimension of the overlying fissures in shallow coal seams has more significant fluctuation characteristics. The reason for this difference deserves further study.
(2) Under the condition of reduced mining height, the fractal dimension of similar simulations begins to fluctuate about 40 m ahead of full-thickness mining. The difference in excavation speed and the amount of mining space are possible influencing factors. According to the fractal dimension curve, the fluctuation characteristics show that there are also differences in the amplitude of the fractal dimension of the two times. The small-amplitude change of the mining thickness may cause the butterfly effect on the overburden fracture [29]. It is speculated that the mining overburden fracture may be a chaotic system.
(3) Dynamic processing of the separation space is of great significance to the control of WF. Chinese scholars have proposed and practiced the grouting and filling technology in the separation space [30]. However, the positioning of the abscission space and the coordinating time and space of grouting and mining have not yet been solved well. Similar simulations are the most feasible among existing methods when studying separation filling technology, but the cost is prohibitive. Numerical simulation has a good advantage in repeating experiments, but it is difficult to characterize the separation space with finite element analysis, and it is difficult to express the grouting and filling effect in block discrete element software. Therefore, the modeling and quantitative analysis of the evolution and control of the separation space by numerical simulation is an important exploration direction.

7. Conclusions

The main conclusions are as follows:

(1) Reducing mining height is an important technical means for safe mining under gullies, and the fractal dimension can describe the confusion of overlying fissures caused by different mining heights. The evolution process of overlying fissures in shallow coal seams can be divided into three stages according to the change law of fractal dimension: rising dimension, fluctuation, and stable stage.
(2) Reviewing the prediction equation for the DHWF shows that the prediction equation for the height of the WF in the western mining area needs to be classified and regressed in combination with the specific overlying rock type, mining thickness, mining intensity, and other parameters to ensure the accuracy of the prediction.
(3) The control of the separation space in the overlying rock is the key to avoiding the sudden increase of the WF height. The fluctuation process of the fractal dimension is consistent with the occurrence and disappearance of the separation space of the overlying rock.

Author Contributions: Conceptualization, K.M. and S.T.; methodology, W.L., X.L. and Y.L.; software, W.L. and L.T.; validation, J.M., L.T., H.Z. and H.T.; formal analysis, K.M. and H.Z.; writing—original draft preparation, K.M.; writing—review and editing, S.T. and H.T.; project administration, S.T. All authors have read and agreed to the published version of the manuscript.

Funding: This research was funded by the National Natural Science Foundation of China (Nos. 51874281), the National Natural Science Foundation for Young Scientists of China (Nos. 52004270).

Institutional Review Board Statement: Not applicable.

Informed Consent Statement: Not applicable.

Data Availability Statement: Data sharing is not applicable.

Acknowledgments: I am very grateful for the support of the research team and the generous help of the engineering and technical staffs of Selian Coal Mine.

Conflicts of Interest: The authors declare no conflict of interest.

Glossary

H_{li}	development height of the water-conducting fracture, m
M	mining height, m
c_i	the coefficient that depends on strata lithology
k	the coefficient in Equation (4)
L	the working face inclination length, m
b	the hard rock proportion coefficient
H	the burial depth, m
Σh	the cumulative total thickness of the hard rock in the overlying rock, m
V	the daily mining speed, m
K_J	the water-resistance coefficient of the bedrock
H_J	the thickness of water-resistance bedrock, m
C_l	the geometric similarity ratio
C_γ	the bulk density similarity constant
C_σ	the stress similarity constant
C_t	the time similarity constant
WF	water-conducting fracture
DHWF	development height of the water-conducting fracture
CIAS	Crack Information Analysis System

References

1. Peng, S.; Bi, Y. Strategic consideration and core technology about environmental ecological restoration in coal mine areas in the Yellow River basin of China. *J. China Coal Soc.* **2020**, *45*, 1211–1221.
2. Wang, C.; Zhang, C.; Zhao, X.; Liao, L.; Zhang, S. Dynamic structural evolution of overlying strata during shallow coal seam longwall mining. *Int. J. Rock Mech. Min. Sci.* **2018**, *103*, 20–32. [CrossRef]
3. Miao, K.; Wang, D.; Tu, S.; Tu, H.; Zhu, D.; Liu, X.; Li, W.; Tang, L. The Principle and Practice of Strong Mine Pressure Control in the Initial Mining and Caving Stages under Multiple Key Strata. *Sustainability* **2022**, *14*, 5772. [CrossRef]
4. Ma, D.; Bai, H. Groundwater inflow prediction model of karst collapse pillar: A case study for mining-induced groundwater inrush risk. *Nat. Hazards* **2015**, *76*, 1319–1334. [CrossRef]
5. Ma, D.; Duan, H.; Li, X.; Li, Z.; Zhou, Z.; Li, T. Effects of seepage-induced erosion on nonlinear hydraulic properties of broken red sandstones. *Tunn. Undergr. Space Technol.* **2019**, *91*, 102993. [CrossRef]
6. Fan, G.; Zhang, D. Mechanisms of Aquifer Protection in Underground Coal Mining. *Mine Water Environ.* **2015**, *34*, 95–104. [CrossRef]
7. Zhang, D.; Fan, G.; Ma, L.; Wang, X. Aquifer protection during longwall mining of shallow coal seams: A case study in the Shendong Coalfield of China. *Int. J. Coal Geol.* **2011**, *86*, 190–196. [CrossRef]
8. Zhang, D.; Fan, G.; Liu, Y.; Ma, L. Field trials of aquifer protection in longwall mining of shallow coal seams in China. *Int. J. Rock Mech. Min. Sci.* **2010**, *47*, 908–914. [CrossRef]
9. Wang, F.; Tu, S.; Zhang, Y.; Song, Q.; Yan, R.; Duan, C. Ground pressure rules and roof control technology for the longwall mining of shallow seam beneath the gully topography. *J. Min. Saf. Eng.* **2015**, *32*, 877–882.
10. Zhang, C.; Tu, S.; Zhao, Y. Compaction characteristics of the caving zone in a longwall goaf: A review. *Environ. Earth Sci.* **2019**, *78*, 27. [CrossRef]
11. Bai, Q.; Tu, S. A General Review on Longwall Mining-Induced Fractures in Near-Face Regions. *Geofluids* **2019**, *2019*, 3089292. [CrossRef]
12. Qian, M.; Shi, P.; Xu, J. *Underground Pressure and Strata Control*; China University of Mining and Technology Press: Xuzhou, China, 2010.
13. Bai, Q.; Tu, S.; Wang, F.; Zhang, X.G.; Tu, H.S.; Yuan, Y. Observation and Numerical Analysis of the Scope of Fractured Zones Around Gateroads Under Longwall Influence. *Rock Mech. Rock Eng.* **2014**, *47*, 1939–1950. [CrossRef]
14. Qian, M.; Xu, J. Behaviors of strata movement in coal mining. *J. China Coal Soc.* **2019**, *44*, 973–984.
15. Mandelbrot, B.B. The Fractal Geometry of Nature. *Am. J. Phys.* **1998**, *51*, 468. [CrossRef]

16. Xie, H.; Yu, G.; Yang, L.; Zhang, Y. Research on the fractal effects of crack network in overburden rock stratum. *Chin. J. Rock Mech. Eng.* **1999**, *18*, 147–151.
17. Xie, H. *Fractals in Rock Mechanics*; CRC Press: Boca Raton, FL, USA, 1993.
18. Wang, Z.; Zhou, H.; Xie, H. Research on fractal characterization of mined crack network evolution in overburden rock stratum under deep mining. *Rock Soil Mech.* **2009**, *30*, 2403–2408.
19. Fan, G.; Zhang, D.; Chen, M.; Zhang, S. Dissipative structure feature of mining fractured overburden system and threshold effect of catastrophic instability. *J. Min. Saf. Eng.* **2019**, *36*, 1093–1101.
20. Guo, L.; Cheng, H.; Seng, S.; Fu, B. Study on Evolution and Subsidence Fractal Characteristics of Overlying Strata in Thick Loose Layers and Thin Bedrocks. *Saf. Coal Mines* **2020**, *51*, 59–64.
21. State Bureau Of Coal Industry. *Regulations for Setting Coal Pillar and Mining Pressed Coal Under Buildings, Water Bodies, Railways, and Main Roadways*; Coal Industry Publishing House: Beijing, China, 2017.
22. Peng, S.S. *Longwall Mining*; CRC Press: Boca Raton, FL, USA, 2019.
23. Fan, L.; Sun, K.; Li, C.; Ning, K.; Ji, R. Thoughts on mine water control and treatment in Yushen mining area. *Coal Geol. Explor.* **2021**, *49*, 182–188.
24. He, X.; Zhao, Y.; Zhang, C.; Han, P. A Model to Estimate the Height of the Water-conducting Fracture Zone for Longwall Panels in Western China. *Mine Water Environ.* **2020**, *39*, 823–838. [CrossRef]
25. Ju, M.; Wang, D.; Shi, J.; Li, J.; Yao, Q.; Li, X. Physical and numerical investigations of bedding adhesion strength on stratified rock roof fracture with longwall coal mining. *Geomech. Geophys. Geo-Energy Geo-Resour.* **2021**, *7*, 24. [CrossRef]
26. Yang, B.; Liu, Y. Application of Fractals to Evaluate Fractures of Rock Due to Mining. *Fractal Fract.* **2022**, *6*, 96. [CrossRef]
27. Tang, C.; Zhu, C.; Cheng, Q.; Zeng, H.; Xu, J.; Tian, B.; Shi, B. Desiccation cracking of soils: A review of investigation approaches, underlying mechanisms, and influencing factors. *Earth-Sci. Rev.* **2021**, *216*, 103586. [CrossRef]
28. Tang, C.; Shi, B.; Liu, C.; Zhao, L.; Wang, B. Influencing factors of geometrical structure of surface shrinkage cracks in clayey soils. *Eng. Geol.* **2008**, *101*, 204–217. [CrossRef]
29. Parmesan, C.; Yohe, G. A globally coherent fingerprint of climate change impacts across natural systems. *Nature* **2003**, *421*, 37–42. [CrossRef] [PubMed]
30. Zhang, L.; Xu, J.; Xuan, D.; Gan, M. Experimental and applied research on compression properties of slurry used for isolated overburden grout injection. *J. China Coal Soc.* **2017**, *42*, 1117–1122.